Available online at www.sciencedirect.com
ScienceDirect
Ceramics International 34 (2008) 787–791
CERAMICS INTERNATIONAL
www.elsevier.com/locate/ceramint

Electric-field-induced strain in Mn-doped $KNbO_3$ ferroelectric ceramics

K. Matsumoto, Y. Hiruma, H. Nagata, T. Takenaka *

Department of Electrical Engineering, Faculty of Science and Technology, Graduate School of Tokyo University of Science, 2641 Yamazaki, Noda, Chiba 278-8510, Japan

Available online 4 October 2007

Abstract

Potassium niobate, $KNbO_3$ (KN), ceramics doped with manganese (Mn) were prepared by a modified conventional ceramic fabrication process to characterize their dielectric, ferroelectric and electrostrain properties. In this study, 0.22% of a large electric-field-induced strain was obtained at 80 kV/cm under unipolar driving for 1.2 wt% $MnCO_3$-doped KN ceramics. Basically, it is difficult to obtain dense and nondeliquescent KN ceramics by the conventional method because of potassium ions. The key factor in obtaining dense and nondeliquescent KN ceramics is the calcination process control. Thus, the two-step calcination pattern is proposed for this purpose. Dense, nondeliquescent and high-resistivity Mn-doped KN ceramics were obtained, resulting in a large electric-field-induced strain under a high electric field.

Keywords: C. Ferroelectric properties; D. Perovskites; E. Actuators; $KNbO_3$

1. Introduction

Lead-free materials have recently have been in demand owing to environmental protection concerns. Candidate materials for lead-free piezoelectric ceramics include $BaTiO_3$ (BT), $(Bi_{1/2}Na_{1/2})TiO_3$ (BNT), $(Bi_{1/2}K_{1/2})TiO_3$ (BKT), $(Na_{1/2}K_{1/2})NbO_3$ (NKN) and $KNbO_3$ (KN) [1–4]. Potassium niobate, $KNbO_3$, has an orthorhombic symmetry at room temperature (RT) and has phase transitions at −10, 225 and 435 °C corresponding to rhombohedral → orthorhombic → tetragonal → cubic phases, respectively [5]. KN ceramics have attracted much attention as one of the candidate materials for lead-free piezoelectric applications, because single-crystal KN has a large piezoelectricity and a high Curie point [6,7]. The electromechanical coupling factor of the thickness-extensional mode, k_t, in a KN crystal reaches as high as 0.69 for the 49.5°-rotated *X*-cut about the *Y*-axis, which is the highest among current lead-free piezoelectrics. There have been many reports on KN solid-solution systems such as $KNbO_3$–$NaNbO_3$ (KNN). Good piezoelectric properties, such as a large planar coupling factor, $k_p = 0.56$, and a large remanent polarization, P_r, up to 30 μC/cm^2, have been observed for KNN ceramics [8]. An excellent piezoelectric property of 416 pC/N in textured $(K_{0.5}Na_{0.5})NbO_3$-based ceramics has recently been reported by Saito et al. [9]. However, because of the poor sinterability of $KNbO_3$ ceramics using conventional firing methods in air, there are few papers and a limited number of reports on the electrical properties of KN ceramics [8,10–12]. The hot-press method has been utilized to obtain a dense ceramic body [13]. On the other hand, Toda et al. has prepared a submicron starting powder using an aqueous solution and dense KN ceramics were obtained by ordinary firing [14]. In addition, it was reported that co-doping of a small amount of Bi_2O_3 and $MnCO_3$ enabled the realization of dense ceramic bodies (more than 97% of theoretical density) by ordinary sintering. However, Bi_2O_3 decreased the piezoelectricity of KN ceramics [15] substantially. On the other hand, recently, the authors have reported the piezoelectric properties of pure $KNbO_3$ piezoelectric ceramics [3]. In the recent report, the authors partially clarified the potential of KN-based lead-free piezoelectric ceramics. In this paper, electric-field-induced strain in Mn-doped KN ceramics, in particular, was investigated to estimate actuator application performance. Also, the dielectric, ferroelectric properties and microstructures were examined.

2. Experimental procedure

Mn-doped $KNbO_3$ ceramics were prepared using the conventional ceramic fabrication process. The prepared

* Corresponding author. Tel.: +81 4 7122 9539; fax: +81 4 7123 0856.
E-mail address: tadashi@ee.noda.tus.ac.jp (T. Takenaka).

0272-8842/$34.00
doi:10.1016/j.ceramint.2007.09.026

compositions were $KNbO_3$ and $MnCO_3$-doped $KNbO_3$ (KN–Mnx). 3N grade powders of K_2CO_3, Nb_2O_5 and $MnCO_3$ were used as starting materials. Equimolar amounts of K_2CO_3 and Nb_2O_5 powders were weighed and put into a 500 ml polyethylene jar. The total mixture was 80 g. These powders were mixed with ethanol and the mixed sizes of zirconia balls (300 g for 2 mm in diameter and 100 balls for 10 mm in diameter) for 24 h. The mixture was dried and then the powders were uniaxially pressed into pellets (30 mm in diameter) at 50 MPa. Prior to the subsequent calcination, these pellets were dried at 200 °C for 6 h. They were heated up to 600 °C at a rate of 100 °C/h and maintained at that temperature for 4 h for the purpose of eliminating residual carbon and forming a $KNbO_3$ structure (first stage). Then the pellets were heated up to 1000 °C and maintained at that temperature for 4 h to be reacted completely (second stage). The cooling rate was 200 °C/h. Calcined pellets were ground, and then ball-milled for 24 h in the same manner as before calcination. After ball-milling, the slurry was dried on a heater.

Then, the dried powder and $MnCO_3$ were weighed to obtain the target compositions ($KNbO_3$ + $x$wt% $MnCO_3$) and mixed by ball-milling with 2-mm zirconia balls for 24 h. After drying, the powder was sieved through a 425 μm mesh sieve. The powder was pressed into pellets of 20 mm in diameter followed by cold-isostatic pressing (CIP) at 150 MPa. These pellets were sintered from 1030 to 1060 °C for 2 h at a heating rate of 100 °C/h and a cooling rate of 200 °C/h in air. The sintering temperature of KN is very close to the melting point; therefore, very careful temperature control was required during sintering. Densities were measured by Archimedes' technique. The sintered samples were characterized using an X-ray diffractometer (Rigaku, RINT2000). A scanning electron microscope (SEM; Hitachi, S-2400) was used to observe the microstructure. For electrical characterization measurements such as those of dielectric and ferroelectric properties, resistivitiy and electric-field-induced strain, the samples were electroded with silver paste. Resistivity was measured using an HP 4329A high resistance meter for 5 mm × 5 mm × 0.5 mm samples. The dielectric constant (ε_s) and dielectric loss (tan δ) dependences on temperature T data were investigated at 10 kHz in the temperature range from RT to 500 °C using an HP 4275A LCR meter for 5 mm × 5 mm × 0.5 mm samples. P–E hysteresis loops were measured for 2 mm × 2 mm × 0.5 mm samples at RT. The applied electric-field frequency was fixed at 0.1 Hz. The induced charge was detected by a charge amplifier (POEL-101). The field-induced-strain was measured using a contact-type displacement sensor (Millitron: Model 1240) at RT and 0.1 Hz.

3. Results and discussion

All of the sintered ceramics were exposed to water with ultrasonic vibrations. Any sintered ceramics showed nondeliquescence. Therefore, the densities of the obtained ceramics were measured by Archimedes' method. All of the ceramics obtained had a ratio of relative density to theoretical density of more than 94%.

Table 1
Optimized sintering temperatures of KN–Mnx (x = 0.05–1.6)

Sample	Optimized sintering temperature (°C)
KN–Mn0.05	1057
KN–Mn0.2	1050
KN–Mn0.4	1045
KN–Mn0.6	1040
KN–Mn0.8	1030
KN–Mn1.2	1030
KN–Mn1.6	1030

Table 1 shows the optimized sintering temperatures of KN–Mnx. Optimized sintering temperature decreased, and it saturated at $x = 0.8$. Fig. 1 shows the compositional dependences of relative density in the KN–Mnx system. These results indicate that an increase in doped-Mn content hinders the realization of a dense ceramic body.

The crystal structure of KN–Mnx (x = 0.05–1.6) was determined from X-ray diffraction (XRD) patterns in Fig. 2. All of the sintered ceramics exhibited orthorhombic peak splitting in XRD patterns. No relationship between Mn content and crystal structures was found. In addition, the differences of the lattice constants were not enough to discuss anything compared with the precision of our XRD equipment.

Fig. 3 shows the microstructure of fractured samples of KN–Mnx (x = 0.05, 0.2, 0.4, 1.6). All of the samples had approximately 2–3 μm cubic grains. On the other hand, any major difference in microstructure with Mn content was not be detected.

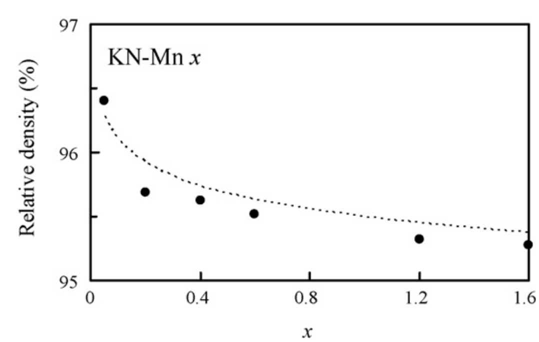

Fig. 1. Compositional dependence of relative density for KN–Mnx system.

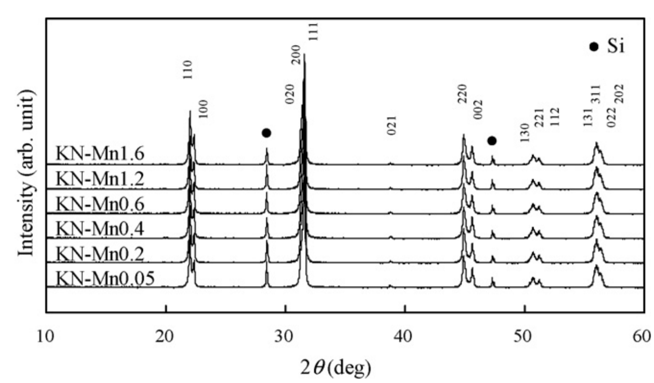

Fig. 2. X-ray diffraction patterns of KN and KN–Mnx (x = 0.05–1.6) ceramics.

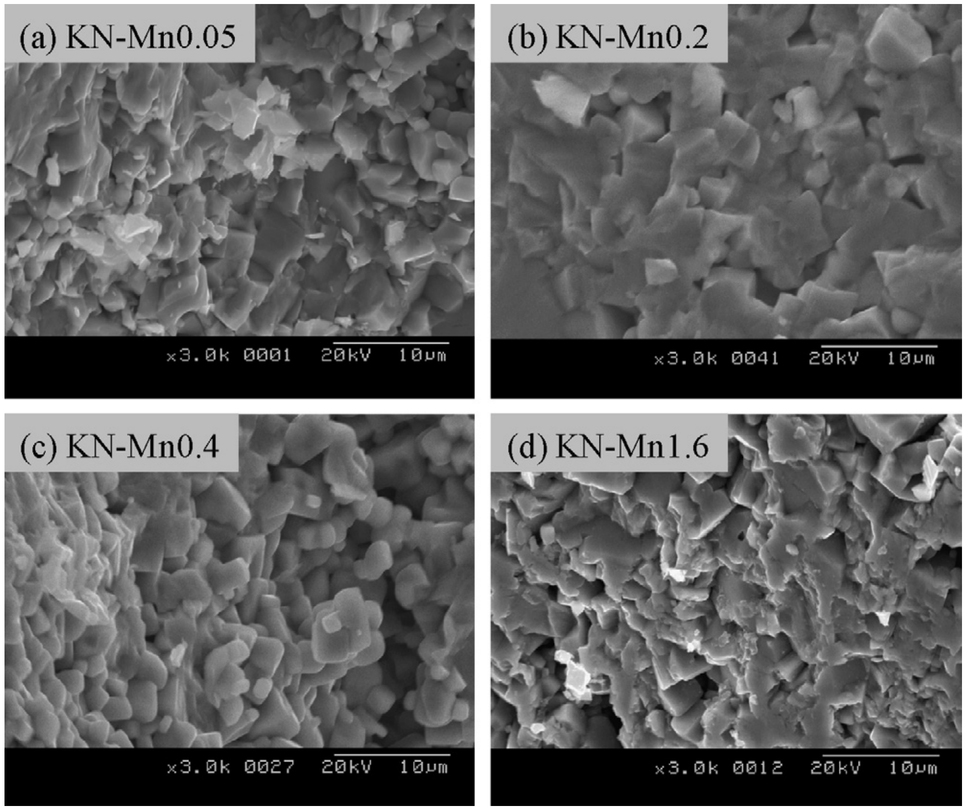

Fig. 3. SEM images of fractured KN–Mnx ceramics. (a) KN–Mn0.05, (b) KN–Mn0.2, (c) KN–Mn0.4, and (d) KN–Mn1.6.

Fig. 4 shows the temperature dependence of dielectric constant ε_s and dielectric loss tan δ for KN–Mnx (x = 0.05–1.6). The ε_s peaks at the Curie tempemperature T_c were sharp. All samples had approximately the same Curie temperature at approximately 420 °C; however, there is no clear relation between T_c and Mn content. In addition, the difference in the phase transition temperature of orthorhombic to tetra phases at around 230 °C was negligibly small. On the other hand, an increase in Mn content resulted in smaller dielectric constants ε_s in this temperature range.

Fig. 5 shows the P–E hysteresis loops of KN–Mnx ceramics. KN–Mn0.2 shows a well saturated square-shaped loop. Meanwhile, the shape of loops changed to a double-like loop with an increase in the amount of Mn. In particular, KN–Mn0.6–1.6 showed a double loop with the remanent polarization close to zero. Fig. 6 shows the strain behavior. KN–

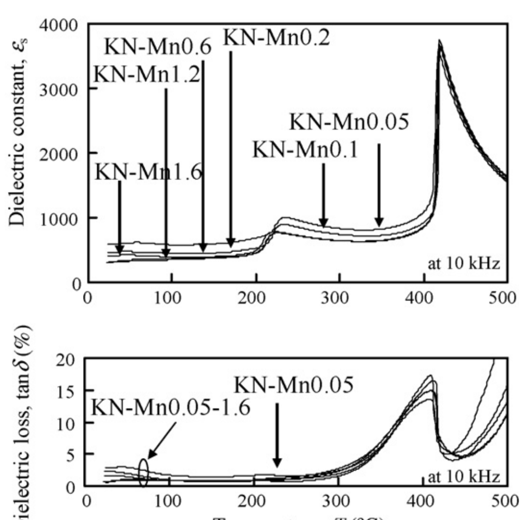

Fig. 4. Temperature dependences of dielectric constant ε_s and loss tangent tan δ for KN–Mnx (x = 0.05–1.6) measured at 10 kHz.

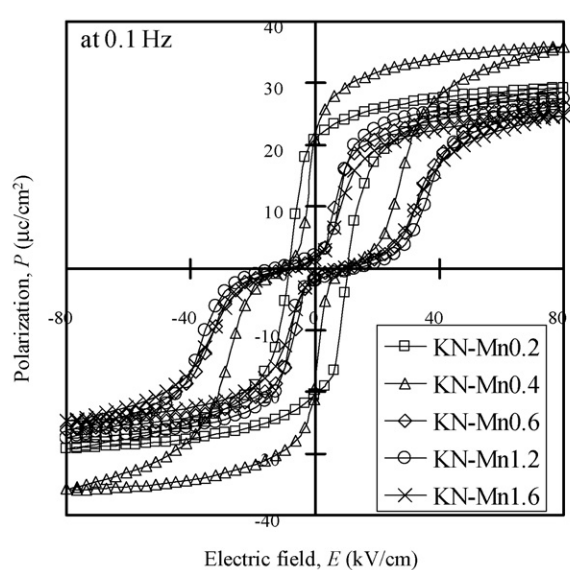

Fig. 5. P–E hysteresis loops of KN–Mnx (x = 0.2, 0.6, 1.2, 1.6).

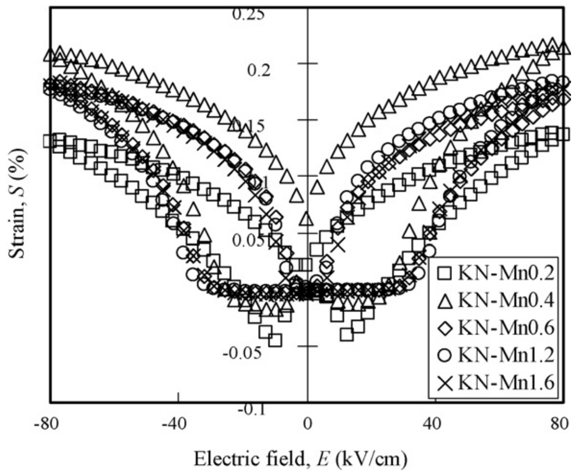

Fig. 6. Bipolar driven S–E properties of KN–Mnx ($x = 0.2, 0.6, 1.2, 1.6$).

Mn0.2 gave a butterfly-shaped loop, such as those of typical piezoelectric materials, with a clear coercive field; in addition, it had a remanent strain at zero electric field. The increase in Mn content changed the shape of the strain loop. KN–Mn0.6–1.6 did not have any E_c and remanent strain.

Fig. 7 shows the strain behavior under unipolar driving in the electric-field range of 0–80 kV/cm. Unipolar driven characteristics are important for actuator devices. KN–Mn0.05 showed small hysteresis in strain; however, it had a relatively small strain for this Mn-doped KN system. The increase in the

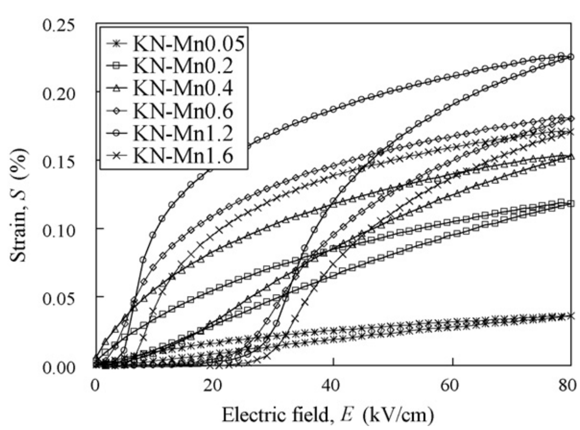

Fig. 7. Unipolar driven strain behavior of KN–Mnx ($x = 0.05$–1.6).

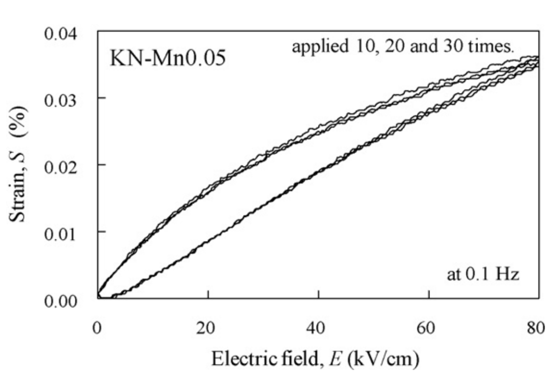

Fig. 8. Fatigue properties S–E curves of KN–Mn0.05 under unipolar driving.

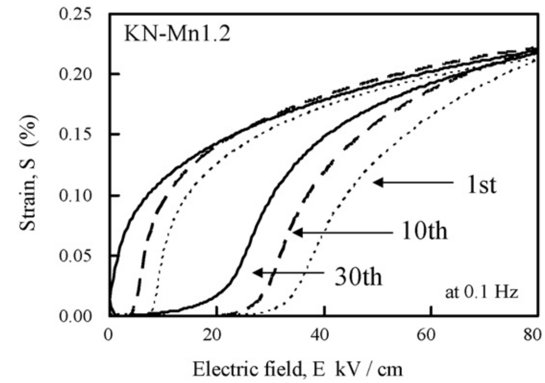

Fig. 9. Fatigue properties S–E curves of KN–Mn1.2 under unipolar driving.

amount of Mn brought a large strain. As a result, the maximum strain was obtained for KN–Mn1.2. The maximum strain of KN–Mn1.2 was 0.22% at 80 kV/cm. This value is relatively large compared with those of other $KNbO_3$-based systems. Fig. 8 shows the fatigue property of S–E curves of KN–Mn0.05. These results indicate that the strain properties were almost the same between the 10th and 30th cycles. The deterioration of this sample was negligible. Fig. 9 shows the aging properties of KN–Mn1.2. Increasing the number of times the electric field is applied reduces the electric field at the rising point of the strain. On the other hand, the maximum strain at 80 kV/cm was almost constant. The advantage of this sample is that the maximum strain is independent of the number of times the electric field is applied. Thus, this sample is suited for developing practical applications.

4. Conclusions

A study on the electrical characterization of Mn-doped $KNbO_3$ ceramics was conducted. Dense and nondeliquescent ceramics were successfully obtained via the ordinary firing method in air by optimizing the fabrication process. Mn-doped KN samples showed relatively large strain compared with other $KNbO_3$-based systems. In particular, unipolar driven KN–Mn1.2 showed a strain of 0.22% under an electric field of 80 kV/cm. This sample showed double-loop P–E hysteresis. On the other hand, KN–Mn0.05 showed relatively small S–E hysteresis, although the maximum strain was the smallest for KN–Mn0.05–1.6. Doping of Mn for KN was effective in obtaining a large resistivity under a high electric field. As a result, a large strain was obtained.

Acknowledgement

This work was partially supported by a Grant-in-Aid for Scientific Research (B) (No. 17360327) from the Japan Society for the Promotion of Science.

References

[1] Y. Hiruma, H. Nagata, T. Takenaka, Phase transition temperatures and piezoelectric properties of $(Bi_{1/2}Na_{1/2})TiO_3$–$(Bi_{1/2}K_{1/2})TiO_3$–$BaTiO_3$ lead-free piezoelectric ceramics, Jpn. J. Appl. Phys. 45 (2006) 7409–7412.

[2] K. Yoshii, Y. Hiruma, H. Nagata, T. Takenaka, Electrical properties and depolarization temperature of $(Bi_{1/2}Na_{1/2})TiO_3$–$(Bi_{1/2}K_{1/2})TiO_3$ lead-free piezoelectric ceramics, Jpn. J. Appl. Phys. 45 (2006) 4493–4496.
[3] K. Matsumoto, Y. Hiruma, H. Nagata, T. Takenaka, Piezoelectric properties of pure and Mn-doped potassium niobate ferroelectric ceramics, Jpn. J. Appl. Phys. 45 (2006) 4479–4483.
[4] E. Hollenstein, M. Davis, D. Damjanovic, N. Setter, Piezoelectric properties of Li- and Ta-modified $(K_{0.5}Na_{0.5})NbO_3$ ceramics, Appl. Phys. Lett. 87 (2005) 182905.
[5] G. Shirane, R. Newnham, R. Pepinsky, Dielectric properties and phase transitions of $NaNbO_3$ and $(Na,K)NbO_3$, Phys. Rev. 96 (1954) 581–588.
[6] K. Nakamura, T. Tokiwa, Y. Kawamura, Domain structures in $KNbO_3$ crystals and their piezoelectric properties, J. Appl. Phys. 91 (2002) 9272–9276.
[7] S. Wada, A. Seike, T. Tsurumi, Poling treatment and piezoelectric properties of potassium niobate ferroelectric single crystals, Jpn. J. Appl. Phys. 40 (2001) 5690–5697.
[8] L. Egerton, D.M. Dillon, Piezoelectric and dielectric properties of ceramics in the system potassium–sodium niobate, J. Am. Ceram. Soc. 42 (1959) 438–442.
[9] Y. Saito, H. Takao, T. Tani, T. Nonoyama, K. Homma, T. Nagaya, M. Nakamura, Lead-free piezoceramics, Nature 432 (4) (2004) 84–87.
[10] B. Jaffe, W.R. Cook, H. Jaffe, Piezoelectric Ceramics, Academic Press Limited, Bedford, OH, 1971, p. 193.
[11] M. Uniyal, K. Singh, S. Bhatt, R.P. Pant, D.K. Suri, B.S. Semwal, Preparation, characterization and dielectric studies of $K_{1-x}Na_xNbO_3$, Indian J. Pure Appl. Phys. 41 (4) (2003) 305–309.
[12] P. Dubernet, J. Ravez, Dielectric study of $KNbO_3$ ceramics over a large range frequency (10^2–10^9 Hz) and temperature (300–800 K), Ferroelectrics 211 (1998) 51–66.
[13] R.E. Jaeger, L. Egerton, Hot pressing of potassium–sodium niobates, J. Am. Ceram. Soc. 45 (1962) 209–213.
[14] K. Toda, S. Tokuoka, N. Ohtake, K. Uematsu, M. Sato, Reaction mechanism of perovskite $KNbO_3$ in aqueous solution, Trans. Mater. Res. Soc. Jpn. 28 (2003) 353.
[15] T. Yoshida, Y. Hiruma, R. Aoyagi, H. Nagata, T. Takenaka, Processing and electrical properties of $KNbO_3$ ferroelectric dense ceramics added with small amount of Bi_2O_3 and $MnCO_3$, Key Eng. Mater. 301 (2006) 19–22.